High-power quantum-dot-based semiconductor disk laser

M. Butkus,[1] K. G. Wilcox,[1,*] J. Rautiainen,[2] O. G. Okhotnikov,[2] S. S. Mikhrin,[3] I. L. Krestnikov,[3] A. R. Kovsh,[3] M. Hoffmann,[4] T. Südmeyer,[4] U. Keller,[4] and E. U. Rafailov[1]

[1]*School of Engineering, Physics and Mathematics, University of Dundee, Dundee DD1 4HN, UK*
[2]*Optoelectronics Research Centre, Tampere University of Technology, P.O. Box 692, FIN-333101 Tampere, Finland*
[3]*Innolume GmbH, Konrad-Adenauer-Allee 11, 44263 Dortmund, Germany*
[4]*Department of Physics, ETH Zurich, 8093 Zurich, Switzerland*
**Corresponding author: k.g.wilcox@dundee.ac.uk*

Received March 4, 2009; revised April 17, 2009; accepted April 23, 2009;
posted April 28, 2009 (Doc. ID 108356); published May 27, 2009

We demonstrate multiwatt cw output power from an optically pumped quantum-dot semiconductor disk laser. Continuous-wave output power of 4.35 W with 22% slope efficiency was demonstrated at a center wavelength of 1032 nm. This represents an increase in power of 15 times and an increase in slope efficiency of 10 times from the previously published results using Stranski–Krastanow grown quantum dots. An intracavity diamond heat spreader was used for thermal management. The maximum output power was limited by the available pump power, and no sign of thermal rollover was observed. © 2009 Optical Society of America

OCIS codes: 140.7270, 140.5960, 140.3480.

Semiconductor disk lasers (SDLs), also known as vertical external-cavity surface-emitting lasers [1], offer a flexible semiconductor laser solution combining power scaling and excellent beam quality [2] while allowing the advantages of intracavity techniques such as frequency mixing [3] and mode locking [4,5] to be exploited. The SDL architecture has been demonstrated in cw operation with many different quantum-well material systems, with output wavelengths from the UV range to the mid-IR range using direct generation or intracavity frequency mixing [3,6,7]. In the 1 μm spectral region, multiwatt output power InGaAs/GaAs quantum-well SDLs with excellent beam quality have been reported. Output powers up to 12 W with $M^2 \sim 2$ were demonstrated using an intracavity diamond heat spreader [8], and up to 20 W was achieved with $M^2 < 1.1$ using substrate removal [2]. Recently the SDL architecture has been combined with quantum-dot (QD)-based gain materials. Examples of SDLs based on InAs/GaAs submonolayer (SML) and InGaAs Stranski–Krastanow (S–K) grown QDs have both been successfully demonstrated [9,10]. In the previous papers, SML QD SDLs producing output powers of up to 1.4 W at 1040 nm and 0.5 W at 950 nm were reported [9], while S–K QD SDLs were reported to produce a maximum power of 300 mW at 1040 nm and 1210 nm [10]. The authors in [10] claimed that slope efficiency, emission wavelength, and laser threshold were temperature-insensitive. Theoretically, QDs should enable temperature insensitivity owing to the three-dimensional confinement that they provide. QD SDLs provide a large gain in bandwidth owing to the size distribution of the dots. This is potentially advantageous for short pulse generation and broadly tunable cw SDLs.

Here we report an S–K QD SDL producing cw output powers of up to 4.35 W with slope efficiencies up to 22%, representing a significant improvement in maximum output power and slope efficiency of QD SDLs. The maximum output power was limited by the available pump power, and no sign of thermal rollover was observed. This demonstration is an important step toward the power scaling of QD-based SDLs to similar power levels as the quantum well examples.

The gain structure in this work used the S–K QD growth formation mechanism. The whole structure was grown on a GaAs substrate by molecular beam epitaxy under standard conditions. The structure consisted of a 29.5 pair GaAs/$Al_{0.9}Ga_{0.1}As$ distributed Bragg reflector (DBR) grown at a design wavelength of 1040 nm. The reflectivity was calculated to be >99.99% at the design wavelength. The active region, grown on top of the DBR, was $7.5\lambda/2$ long and consisted of five groups of seven QD layers positioned at the antinodes of the E-field standing wave. Each QD layer was formed by cyclically (nine times) depositing InAs (0.06 nm) and GaAs (0.06 nm). The QD layers were separated by 10 nm GaAs spacer layers to minimize material defects [11]. The dot density was $\sim 3 \times 10^{10}$ cm^{-2}. Between the groups of QD layers, GaAs spacers served the dual purpose of being transparent spacers at the laser design wavelength and pump absorber regions for the 808 nm pump light. A 15-nm-thick $Al_{0.9}Ga_{0.1}As$ cap layer was used to prevent surface recombination of the excited carriers. Finally, a 20 nm GaAs cap layer was placed at the semiconductor–air interface to avoid oxidation. The active region was designed at a wavelength of 1040 nm, with the ground-state and excited-state emission of the QD layers centered at 1060 nm and 1020 nm, respectively.

Thermal management is critical to allow power scaling of SDLs. Two main approaches have therefore been developed—the use of a high thermal conductivity intracavity heat spreader [12] and substrate removal [1,13]. The use of a diamond intracavity heat spreader has been demonstrated to be a very flexible approach, utilized in the demonstration of many

0146-9592/09/111672-3/$15.00

novel wavelength SDLs [7]. Two pieces of the gain chip were prepared and investigated, one mounted with no post processing directly onto a thermoelectric temperature-controlled copper heat sink. The second sample was bonded to a 293-μm-thick type IIa natural diamond intracavity heat spreader using the liquid capillary bonding technique and mounted on the same heat sink to power scale the QD SDL output [14]. The top surface of the diamond was antireflective coated for both the pump and laser wavelengths.

The gain structures were optically pumped with pump spot diameter of 120 μm using a 20 W, 808 nm, and 100 μm diameter core fiber-coupled diode laser. The samples were tested in both a two-mirror straight cavity and in a V-cavity configuration. In the straight cavity the gain formed one end of the cavity, and an output coupler of −75 mm radius of curvature formed the other. The V cavity was formed with the gain as one end mirror, a −100 mm radius of curvature high reflector as the folding mirror, and a plane output coupler closing the cavity (see Fig. 1). In both cases several different transmission output couplers were used to find the optimal output coupling. The output power was measured using a calibrated power meter, the beam profile was measured using a Dataray WinCam-D CCD-based beam profiler, and the output spectra was measured using a 0.01 nm resolution fiber-coupled spectrometer.

The unprocessed sample produced a maximum output power of 100 mW centered at a wavelength of 1050 nm, with the heat-sink temperature set to 5°C in the straight cavity. A 0.15% output coupler was used, and an incident pump power of 1 W was used before thermal rollover occurred. The threshold pump power was 2.5 kW/cm^2, and the slope efficiency was 12%. As the heat-sink temperature was increased, the slope efficiency and maximum output power fell rapidly; at 20°C, the slope efficiency was 6%, and the maximum output power was 22 mW with 0.9 W incident.

When the sample with the intracavity diamond heat spreader was tested, a maximum output power of 4.35 W was achieved at a heat-sink temperature of 5°C. The slope efficiency was measured to be 22%, and the optical spectrum was centered at 1032 nm, coinciding with the excited-state emission of the QDs. The laser output was linearly polarized with a horizontal orientation in all cases. At a heat-sink temperature of 15°C a maximum output power of 4 W was observed, and the slope efficiency slightly decreased to 19%. These output powers were observed when an optimum output coupling of 1% was used. It is important to note that the observed output power was limited by the available pump power. No sign of thermal rollover was observed, and hence power scaling above the 4 W mark should be straightforward with a more powerful pump source. The diamond heat spreader QD SDL input–output power characteristics and optical spectra at different pump powers are shown in Fig. 2. The distinct periodically spaced peaks in the output spectra were caused by the spectral filtering induced by the etalon formed by the intracavity diamond heat spreader.

The output beam quality was measured using a standard Z-scan technique with a CCD-based beam profiler to obtain the beam quality factor (M^2). The laser cavity design allowed increased control over the cavity mode and produced a low-divergence output. The cavity lengths were 58 mm between the gain mirror and the curved high reflector and 156 mm between the high reflector and the output coupler. This cavity configuration ensured optimal overlap of the laser cavity mode and the pump beam spot. Output couplers of 0.15% and 0.6% were used with the unprocessed sample and with the diamond heat spreader sample, respectively, and in both cases the heat-sink temperature was set to 5°C. The unprocessed sample produced 50 mW output power in a circularly symmetric Gaussian beam with M^2=1.1. The

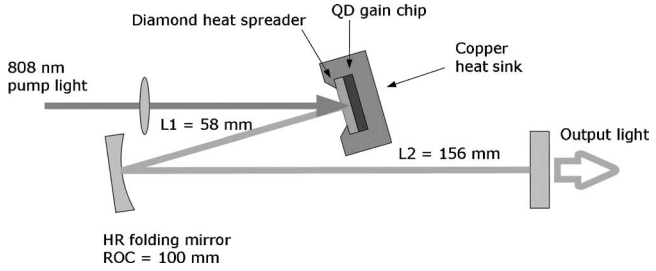

Fig. 1. Schematic of the V-cavity laser configuration.

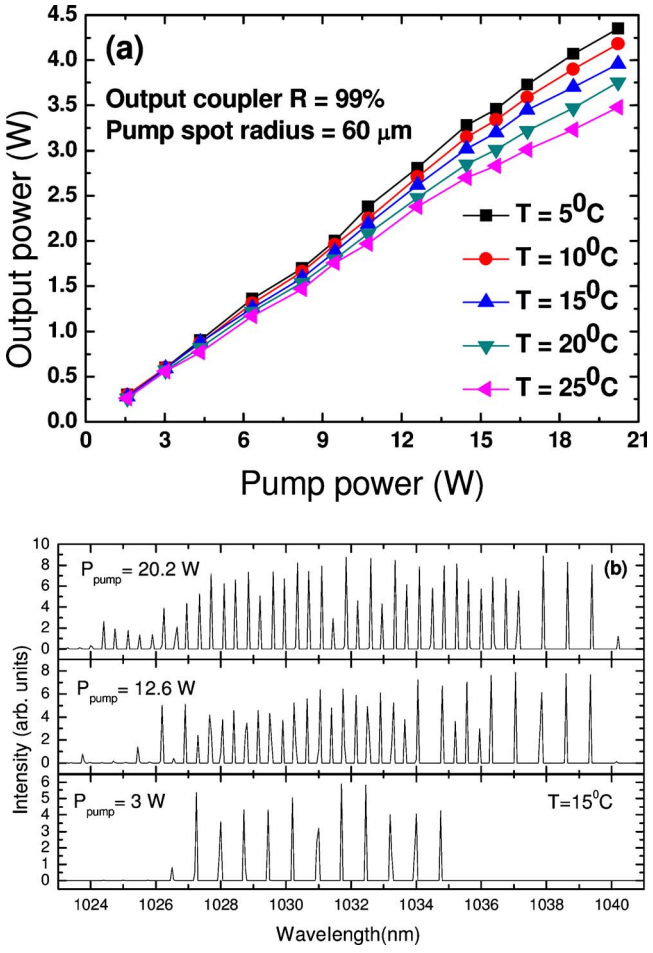

Fig. 2. (Color online) (a) Output power versus pump power characteristics of diamond heat spreader SDL. (b) Optical spectra of the same sample at different pump powers.

diamond heat spreader sample demonstrated up to 3 W power with a circularly symmetric near-Gaussian beam, which became somewhat multimode at high output power. At 3 W output, the beam quality was measured to be $M^2=3.5$. With a lower output power of 0.5 W, a beam quality of $M^2=1.5$ was measured. Output beam intensity profiles for both the unprocessed and the diamond heat spreader samples are shown in Fig. 3. In the case of highest output power of 4.35 W in a straight cavity, M^2 was measured to be 4.5.

The observed rapid decrease in the slope efficiency of the unprocessed sample with increasing heat-sink temperature shows that this structure is temperature sensitive. The physical cause of this temperature dependence is under investigation, but we believe it is due to coupling of the carriers between the QDs and the wetting layers. The more efficient thermal management in the sample with the diamond heat spreader reduced the pump-induced temperature increase of the gain region and hence allowed the gain to operate farther from thermal rollover. This reduced the sensitivity of the slope efficiency to the heat-sink temperature in this sample.

Finite-element analysis has previously shown a ~50 K temperature rise in the center of the pump spot compared to the edge in a QW SDL with an diamond heat spreader and similar pump conditions [12]. We believe that this spatial temperature variation causes a spatially varying gain profile as the QDs in the center of the gain spot exhibit thermal rollover. This gain profile supports higher-order modes in preference to the fundamental Gaussian cavity mode and causes the laser beam quality degradation at higher pump powers than we observed.

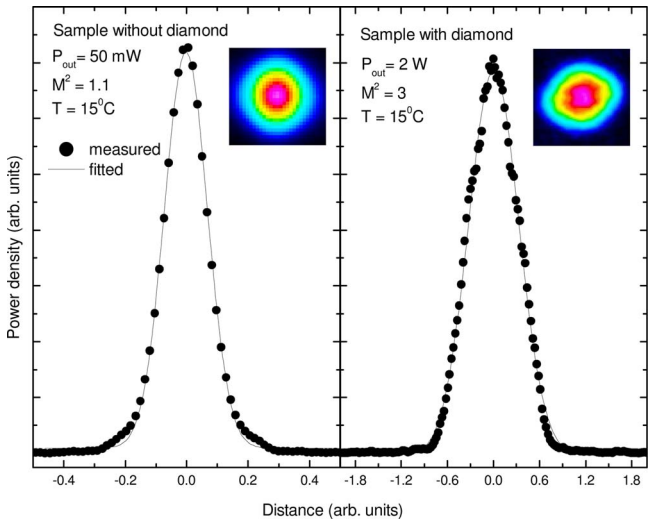

Fig. 3. (Color online) Intensity profiles of the output beam characterized with the unprocessed sample (left) and the diamond heat spreader sample (right) in a V-cavity configuration.

We demonstrate pump-power-limited cw output powers of up to 4.35 W from an optically pumped Stranski–Krastanow QD semiconductor disk laser using an intracavity diamond heat spreader. This represents an increase in power of 15 times from the previously published result using S–K QDs [9], and is the first multiwatt output from any QD SDL (to our knowledge). The experimental demonstration of a multiwatt power level cw operation of QD-based SDLs is an important step to producing watt-level QD-based, mode-locked, and broadly tunable cw SDLs.

The research leading to these results has received funding from the European Community's Seventh Framework Programme (FAST-DOT) under grant agreement 224338.

References

1. M. Kuznetsov, F. Hakimi, R. Sprague, and A. Mooradian, IEEE J. Sel. Top. Quantum Electron. **5**, 561 (1999).
2. B. Rudin, A. Rutz, M. Hoffmann, D. J. H. C. Maas, A.-R. Bellancourt, E. Gini, T. Sudmeyer, and U. Keller, Opt. Lett. **33**, 2719 (2008).
3. J. E. Hastie, L. G. Morton, A. J. Kemp, A. B. Krysa, J. S. Roberts, and M. D. Dawson, Appl. Phys. Lett. **89**, 061114 (2006).
4. U. Keller and A. C. Tropper, Phys. Rep. **429**, 67 (2006).
5. K. G. Wilcox, Z. Mihoubi, G. J. Daniell, S. Elsmere, A. Quarterman, I. Farrer, D. A. Ritchie, and A. Tropper, Opt. Lett. **33**, 2797 (2008).
6. J. M. Hopkins, R. D. Preston, A. J. Maclean, S. Calvez, H. Sun, J. Ng, M. Steer, M. Hopkinson, and D. Burns, J. Mod. Opt. **54**, 1677 (2007).
7. A. C. Tropper, H. D. Foreman, A. Garnache, K. G. Wilcox, and S. H. Hoogland, J. Phys. D **37**, R75 (2004).
8. K. S. Kim, J. Yoo, G. Kim, S. Lee, S. Cho, J. Kim, T. Kim, and Y. Park, IEEE Photonics Technol. Lett. **19**, 1655 (2007).
9. T. D. Germann, A. Strittmatter, U. W. Pohl, D. Bimberg, J. Rautiainen, M. Guina, and O. G. Okhotnikov, J. Cryst. Growth **310**, 5182 (2008).
10. T. D. Germann, A. Strittmatter, J. Pohl, U. W. Pohl, D. Bimberg, J. Rautiainen, M. Guina, and O. G. Okhotnikov, Appl. Phys. Lett. **93**, 051104 (2008).
11. N. N. Ledentsov, V. A. Shchukin, M. Grundmann, N. Kirstaedter, J. Böhrer, O. Schmidt, D. Bimberg, V. M. Ustinov, A. Y. Egorov, A. E. Zhukov, P. S. Kop'ev, S. V. Zaitsev, N. Y. Gordeev, Zh. I. Alferov, A. I. Borovkov, A. O. Kosogov, S. S. Ruvimov, P. Werner, U. Gösele, and J. Heydenreich, Phys. Rev. B **54**, 8743 (1996).
12. A. J. Kemp, G. J. Valentine, J. M. Hopkins, J. E. Hastie, S. A. Smith, S. Calvez, M. D. Dawson, and D. Burns, IEEE J. Quantum Electron. **41**, 148 (2005).
13. R. Häring, R. Paschotta, A. Aschwanden, E. Gini, F. Morier-Genoud, and U. Keller, IEEE J. Quantum Electron. **38**, 1268 (2002).
14. J. E. Hastie, J. M. Hopkins, S. Calvez, C. W. Jeon, D. Burns, R. Abram, E. Riis, A. I. Ferguson, and M. D. Dawson, IEEE Photonics Technol. Lett. **15**, 894 (2003).